frontiers in Physics

ORIGINAL RESEARCH
published: 29 October 2020
doi: 10.3389/fphy.2020.581519

Perfluorocarbon-Loaded Hydrogel Microcapsules from Interface Shearing for Magnetic Guided Ultrasound and Laser Activation

Zhiqiang Zhu[1,2], *Ming Zhang*[1,2], *Yuanqing Zhu*[1,2], *Fangsheng Huang*[1,2], *Ting Si*[2,3]* and *Ronald X. Xu*[1,2,4]

[1] Department of Precision Machinery and Precision Instrumentation, University of Science and Technology of China, Hefei, China, [2] Key Laboratory of Precision Scientific Instrumentation of Anhui Higher Education Institutes, University of Science and Technology of China, Hefei, China, [3] Department of Modern Mechanics, University of Science and Technology of China, Hefei, China, [4] Department of Biomedical Engineering, The Ohio State University, Columbus, OH, United States

Stimuli-responsive microcarriers have received considerable attention in a variety of fields, including disease diagnosis, drug delivery, sensing, and imaging. Here, we report the generation of multiple-responsive perfluorocarbon-loaded magnetic hydrogel microcapsules (PMHMs) with uniform size for magnetic controlled ultrasound (US) and laser activation. The PMHMs are fabricated by a novel coaxial interface shearing (CIS) method based on the mechanism of liquid bridge formation and fracture. Perfluorocarbon and iron oxide magnetic nanoparticles are used as US-responsive and photothermal absorption medium, respectively, and magnetic nanoparticles are also used for magnetic-controlled targeting. Moreover, the size, structure, and function of the prepared biocompatible PMHMs can be precisely controlled by adjusting the process parameters of CIS. It is indicated that the PMHMs have different US- and light-responsive characteristics, mainly because of the difference of their activation mechanisms. It is demonstrated that laser has better activation resolution and can achieve site-specific activation and drug release of PMHMs. The multiple-responsive features imply that the PMHMs fabricated by CIS may provide an effective drug release platform for biomedical and pharmaceutical applications.

Keywords: microfluidics, microcapsule, drug delivery, ultrasound, laser activation

OPEN ACCESS

Edited by:
Zhaoyu Li,
University of Queensland, Australia

Reviewed by:
Yukun Ren,
Harbin Institute of Technology, China
Lingling Shui,
South China Normal University, China

***Correspondence:**
Ting Si
tsi@ustc.edu.cn

Specialty section:
This article was submitted to Medical Physics and Imaging, a section of the journal Frontiers in Physics

Received: *09 July 2020*
Accepted: *22 September 2020*
Published: *29 October 2020*

Citation:
Zhu Z, Zhang M, Zhu Y, Huang F, Si T and Xu RX (2020) Perfluorocarbon-Loaded Hydrogel Microcapsules from Interface Shearing for Magnetic Guided Ultrasound and Laser Activation. Front. Phys. 8:581519. doi: 10.3389/fphy.2020.581519

INTRODUCTION

The advanced drug delivery system (DDS) can deliver drugs to the target organ, and effectively adjust the physicochemical properties of the drug, to improve treatment effect, reduce toxic and side effects, and save treatment cost [1–5]. As a novel DDS, stimuli-responsive microcarriers (SRMs) can release drugs on demand under stimuli, which can further manipulate drug release behaviors and improve therapeutic effect [4, 5]. The physicochemical properties of SRMs, such as size, structure, shape, and composition are vital for drug release process under stimuli. Commonly used stimuli methods include physical- (such as light, heat, electric field, and ultrasound) and chemical-based stimuli methods (such as enzymes, pH, and glucose). The emerging physical-based stimuli methods such as ultrasound (US) and laser offer a convenient and robust controlled drug release platform and have attracted extensive interest [6–13].

However, most existing SRMs lack precise structural and functional design and control. Meanwhile, the application of SRMs in biomedicine and other fields needs further exploration and research.

The emergence of microfluidic technology provides strong technical support for the preparation of complex emulsions with high controllability over size, structure, and properties, which offers excellent conditions for further preparation of advanced DDS (such as microparticles, microcapsules, and microgels) [14–18]. Generally, commonly used droplet microfluidic devices mainly include glass capillary- [19–24], PDMS- [25–30], metal capillary- [31–39], and 3D printing-based [40–43] devices. According to the mechanism of droplet generation, droplet generation methods are mainly divided into active and passive. Notably, in most commonly used passive droplet generation methods, the physicochemical parameters of the fluids and microfluidic devices all affect the size and uniformity of produced complex emulsions [44–47]. Therefore, it is of considerable significance to develop accurate and reliable methods to prepare SRMs and further explore their applications in biomedicine and other fields.

In this work, an active droplet generation method based on coaxial interface shearing (CIS) [48, 49] was proposed to prepare monodisperse multiple-responsive perfluorocarbon-loaded magnetic hydrogel microcapsules (PMHMs), as illustrated in **Figure 1**. Perfluorocarbon (PFC) was used as a kind of US-responsive agent, and iron oxide magnetic nanoparticles (MNPs) were used as magnetic attraction and light absorption medium in the PNIPAM hydrogel shell. The CIS experimental system was easy to set up and can prepare double emulsions quickly and stably at a very low cost. Based on interface shearing mechanism, the double emulsions were formed when the liquid bridge was pulled off. In addition, the size of the double emulsion was determined only by the flow rate and vibration frequency, and can be accurately controlled in a broad range. By adjusting the relevant experimental parameters, the PFC-loaded NIPAM core-shell droplet with different sizes and structures can be easily prepared. It has been demonstrated that the PMHMs can make directional movement under the control of the external magnetic field. Under the activation of ultrasound or laser, the PFC core underwent a liquid-gas phase transition and expanded rapidly and exploded. These multiple-responsive abilities of the PMHMs open up new possibilities for their practical application in the fields of biology and medicine.

MATERIALS AND METHODS

Materials and Reagents

N-isopropylacrylamide (NIPAM; Mw: 113 g/mol), N,N′-methylenebis (acrylamide) (MBA; Mw: 154 g/mol), 2,2′-azobis (2-methylpropionamidine) dihydrochloride (V50; Mw: 271 g/mol), 2,2-dimethoxy-2-phenylacetophenone (BDK; Mw: 256 g/mol) were purchased from Shanghai Aladdin Biochemical Technology Co., Ltd (Shanghai, China). Span 80, poly (vinyl alcohol) (PVA; Mw: 13,000–23,000 g/mol), Iron oxide (II, III) magnetic nanoparticle (MNPs; Mw: 231 g/mol, 20 nm) was purchased from Shanghai Macklin Biochemical Co., Ltd (Shanghai, China). 1,1,1,2,3,4,4,5,5,5-decafluoropentane (Mw: 252 g/mol, bp: 55°C) were purchased from Sigma-Aldrich LLC (St. Louis, MO, USA). Mineral oil was purchased from Sinopharm Chemical Reagent Co., Ltd (Shanghai, China). Ultrapure deionized water was generated by a Direct-Q® Water Purification System (Merck KGaA, Darmstadt, Germany).

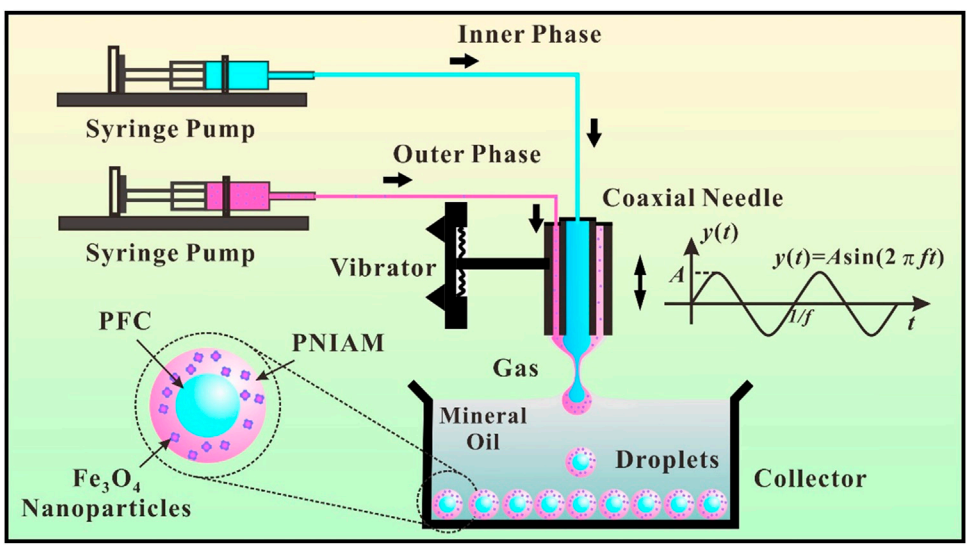

FIGURE 1 | Schematic illustration of an on-demand coaxial interface shearing (CIS) double emulsion generation system including a coaxial needle, two syringe pumps, an electric vibrator, and a collecting pool.

Coaxial Interface Shearing Double Emulsion Generation System

The CIS process can be described as the formation and rupture of a compound liquid bridge for on-demand generation of multiple emulsions when a coaxial needle supplying liquids vibrates periodically across a free gas-liquid surface. Two precision injection pumps (LSP02-2A, Longer Precision Pump Co., Ltd, China) were used to provide inner and outer fluids to the coaxial needle, composed of an inner needle (28G) and an outer needle (21G). The two needles were adjusted to high concentricity under a microscope. A signal generator (DG1022U, RIGOL Electronic, China) was used to generate the excitation waveform, and a power amplifier (SA-PA080, Wuxi Shiao Technology Co., Ltd, China) was used to drive an electric vibrator (JZK-2, SHIAO, China) and the coaxial needle to vibrate. The NIPAM double emulsions were generated during the upward movement of the coaxial needle and sank into the bottom of the quartz pool due to high density. A CCD camera (DFK 23G274, The Imaging Source, LLC, USA) connected to a computer was used to monitor the NIPAM double emulsions generation process from one side of the quartz pool, and a strobe light (3 kHz, PN-01D, Hangzhou Pintoo Electronic Technology Co., Ltd, China) was used to illuminate from the other side of the quartz pool.

Crosslinking Process and Morphology Analysis of Perfluorocarbon-Loaded Magnetic Hydrogel Microcapsules

After the generation of double emulsions, an UV LED light (DSX-UVP60, 365 nm, 9.9 W/cm^2, Shenzhen Deshengxing Electronics Co., Ltd, China) was used to crosslink the NIPAM outer shell. The distance between the light and the samples was set as 20 cm. The collected double emulsions were converted into PMHMs after the UV light irradiation crosslinking for 3 min. Optical images of the PMHMs were achieved by an optical microscope (SZX7, OLYMPUS Corp, Tokyo, Japan). Image-Pro and Origin 2017 software were used to analyze the size of the produced PMHMs. The polydispersity index (PDI) of the double emulsion was calculated by the standard deviation (SD) divided by the mean value of diameter.

Magnetic Controlled Movement and Activation of Perfluorocarbon-Loaded Magnetic Hydrogel Microcapsules

For magnetic controlled movement of PMHMs, the produced PMHMs were placed into a glass rectangular slot (length: 12, width: 2, height: 1 mm) filled with mineral oil. Two cuboid NdFeB magnets (length: 40, width: 20, height: 5 mm) were used to control the movement of the PMHMs. The initial distance between the magnet and the microcapsule was 10 mm. The magnetic attraction process of the PMHMs under magnetic field was recorded by a microscope equipped with a CCD camera (MSX2-H, Mshot Photoelectric Technology Co., Ltd, China).

For US activation of PMHMs, several PMHMs were placed in a 96-well plate filled with mineral oil and coupling agent was applied to the bottom of the well plate. An ultrasonic therapeutic apparatus (UT1041, Shenzhen Dundex Technology Co., Ltd, China) with a probe of 5 cm^2 was used to activate the PMHMs.

For laser activation of PMHMs, several PMHMs were placed in a Petri dish filled with mineral oil. A near-infrared (NIR) laser (808 nm, 0.5 W, Shenzhen Fulei Laser Technology Co., Ltd, China) was used to active the PMHMs. A lens was used to focus the laser to increase the laser energy density, and the PMHM explosion process was also captured by the Mshot CCD.

RESULTS AND DISCUSSION

Coaxial Interface Shearing Process and Analysis

The on-demand CIS double emulsion generation system is illustrated in **Figure 1**. The experimental system mainly consists of three parts: the first part is liquid supply system, the second part is mechanical vibration system, and the last part is droplet generation and collection system. The initial position of the end of the coaxial needle is adjusted to be flush with the liquid level in the quartz pool. The vibration process of the coaxial needle meets the standard sine function, and the vibration amplitude and frequency can be precisely adjusted within a certain range. The double emulsions are generated during the process of the coaxial needle passing through the gas-liquid interface periodically. In a typical NIPAM double emulsions generation process, the inner phase is 1,1,1,2,3,4,4,5,5,5-decafluoropentane. The outer phase is 11.3% (w/v) monomer NIPAM, 10% (w/v) crosslinker MBA, 0.5% (w/v) initiator V50, and 2% (w/v) MNPs dissolved in 10% (w/v) PVA aqueous solution. The stationary phase is mineral oil with 11.3% (w/v) Span 80 and 0.5% (w/v) crosslinker BDK. When the process parameters such as inner and outer flow rates (Q_i, Q_o), vibration frequency (f), and amplitude (A) are suitable, double emulsions can be prepared stably (Supplementary Video 1). It is worth noting that other types of double emulsions (such as W/O/W, O/O/W, and W/W/O) can also be produced by the CIS process [48, 49].

When the coaxial needle contacts the stationary phase, a liquid bridge will be formed between them because of capillary force. The external envelope shape of the liquid bridge satisfies the Young-Laplace differential equation [49]. With the inner and outer phase fluids flowing through the coaxial needle, an inner meniscus and an outer meniscus are formed at the end of the coaxial needle and increase gradually. Before the fracture of the liquid bridge, the resultant force (capillary force, net buoyancy, viscous resistance, inertial force, and mass inertia force) of the droplet needs to satisfy the Newton's second law. As the capillary force is usually dominant, the droplet and the needle can move synchronously before the fracture of the liquid bridge [49]. As the coaxial needle leaves the initial position and rose gradually, the liquid bridge will shrink gradually and break at a certain height (h). The droplets will be produced along with the fracture of the liquid bridge. Theoretically, h is the minimum value of height when the differential equation has no solution. In this experiment, the amplitude of the coaxial

needle is set as 1.35 mm to ensure fracture of the liquid bridge. Under these conditions, the double emulsion can drop off the tip of the needle and sink to the bottom of the quartz pool because of the higher density. In addition, the vibration frequency, flow rate and other parameters need to be controlled within a certain range to ensure the steady operation of CIS process [49]. The produced double emulsions are collected at the bottom of the quartz pool and wait for subsequent processing and application.

Generation and Characterization of Perfluorocarbon-Loaded Magnetic Hydrogel Microcapsules

Figure 2A shows the generation process of PFC-loaded NIPAM double emulsions in mineral oil. The black arrows in the image indicate the coaxial needle and the produced core-shell droplets. Due to the presence of surfactant in mineral oil, the double emulsions can be stably arranged at the bottom of the quartz pool without fusion. The optical microscopic image of the collected uniform double emulsions at the preparation parameters of Q_o = 15 μL/min, Q_i = 15 μL/min, and f = 4 Hz is shown in **Figure 2B**. The black arrows in the image indicate the inner PFC core and outer NIPAM shell before UV light irradiation, and the boundary between the two is evident. The average radii of the inner core and the outer shell are 267.8 and 327.1 μm, and polydispersity indexes are 2.0% and 1.8%, respectively, (**Figure 2C**). After the production of the PFC-loaded NIPAM double emulsions, the UV light is used to crosslink the NIPAM shell to form hydrogel microcapsules. The outer shell changes from colorless to gray, but the size of the double emulsion changes little after crosslinking (**Figure 2D**).

Size Control of Double Emulsions

In a standard CIS process, the generation frequency of the double emulsions equals to the coaxial needle vibration frequency [48, 49]. The relationship between the double emulsion volume (V) and flow rates and frequency can be expressed as follows,

$$V = (Q_i + Q_o)/f,$$

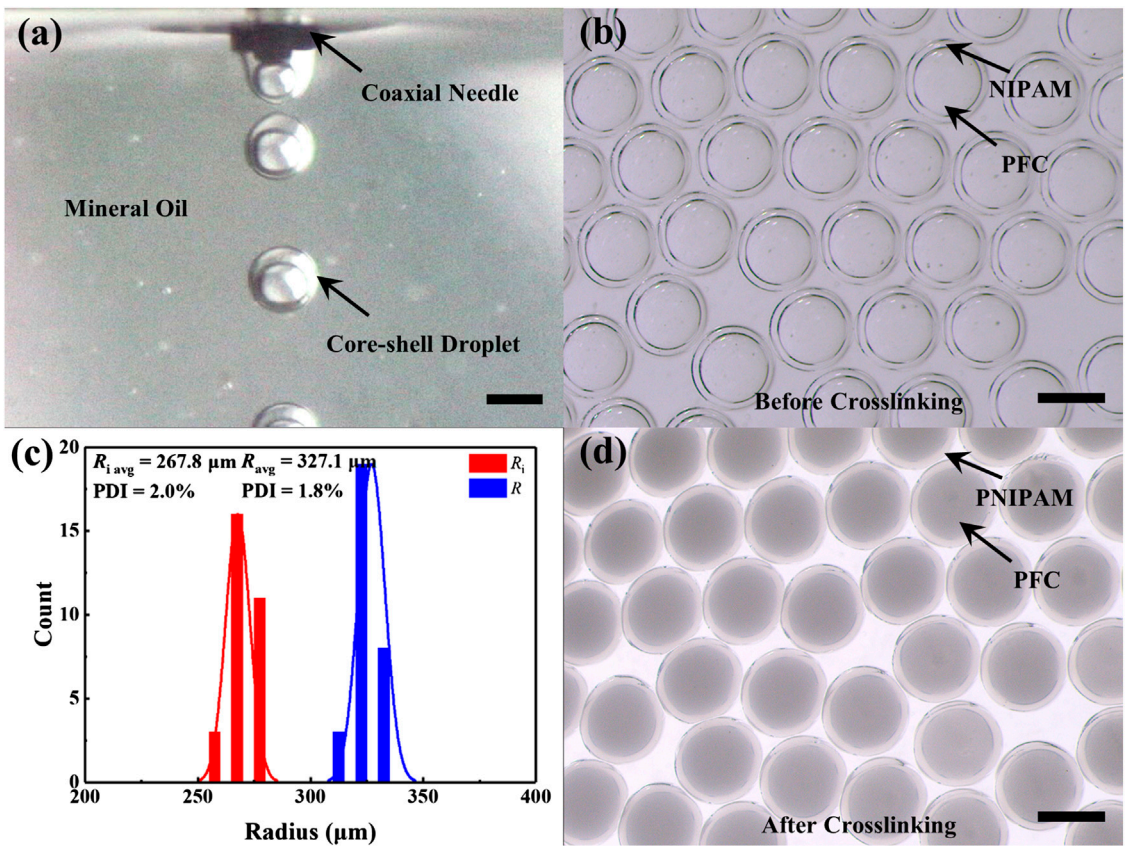

FIGURE 2 | The preparation of PFC-loaded NIPAM double emulsions. **(A)** Real-time CIS process during core-shell droplets formation. **(B)** Optical microscopic image of the produced PFC-loaded NIPAM double emulsions dispersed in mineral oil before crosslinking (Q_o = 15 μL/min, Q_i = 15 μL/min, f = 4 Hz). **(C)** Size distributions of the double emulsions inner core and outer shell in **(B)**. **(D)** The change of the double emulsion morphology after crosslinking (Q_o = 15 μL/min, Q_i = 15 μL/min, f = 4 Hz). Scale bar: 500 μm.

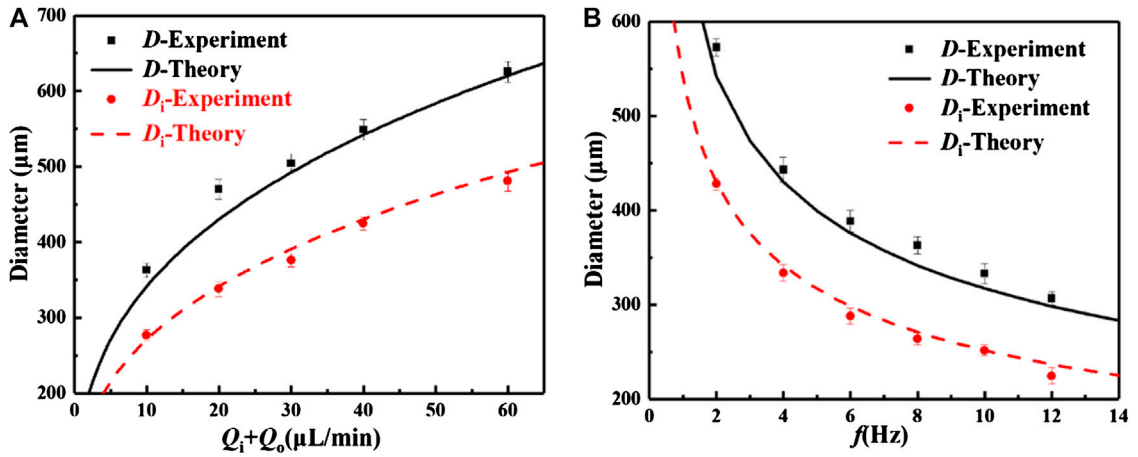

FIGURE 3 | Influence of experimental parameters on the size of the double emulsion. **(A)** The relationships between total flow rate and core and shell sizes (f = 8 Hz, $Q_i = Q_o$). **(B)** The relationships between vibration frequency and core and shell sizes ($Q_i + Q_o$ = 10 μL/min, $Q_i = Q_o$).

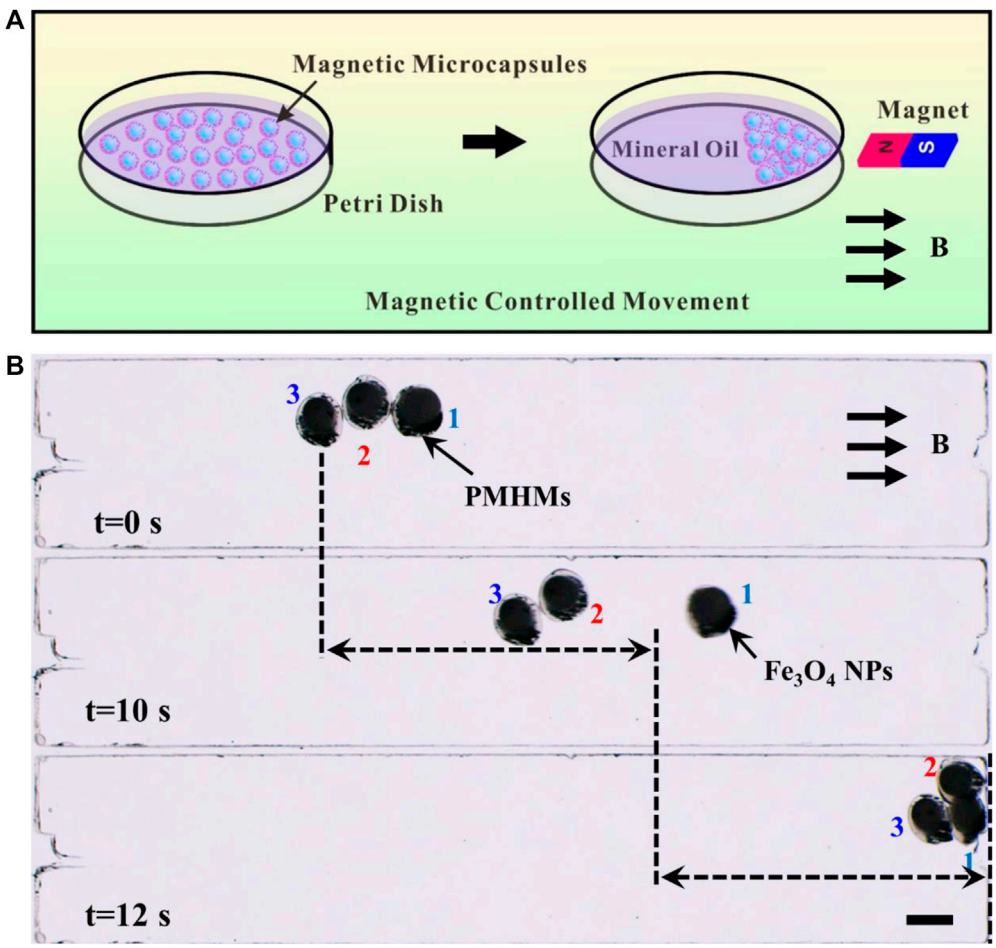

FIGURE 4 | (A) Schematic illustration of magnetic-guided PMHMs. **(B)** The positions of PMHMs at 0, 10, and 12 s under the action of the magnetic field. Scale bar: 500 μm.

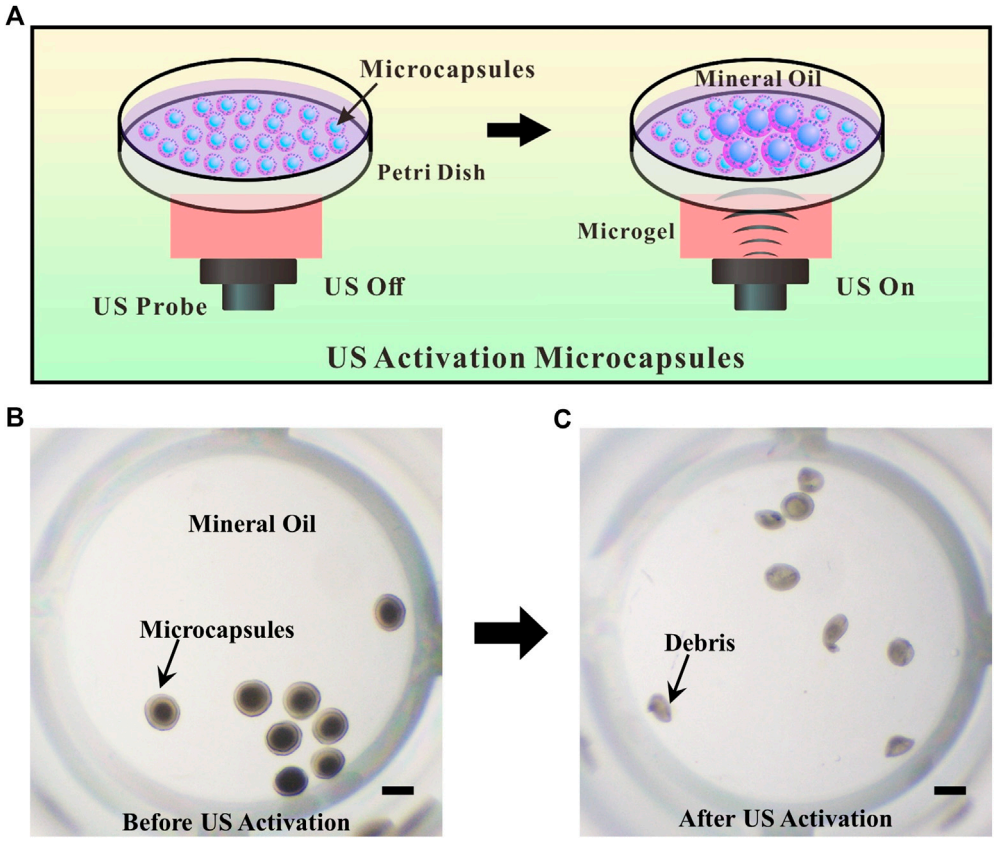

FIGURE 5 | (A) Schematic illustration of US activation of PMHMs. **(B)** Microscopic image of the produced PMHMs in a 96-well plate before US activation. **(C)** Microscopic image of the produced PMHMs after US activation. Scale bar: 500 μm.

Similarly, the relationship between the inner core volume (V_i) and flow rates and frequency can be expressed as follows,

$$V_i = Q_i/f,$$

Therefore, the double emulsion diameter (D) and the inner core diameter (D_i) can be calculated as,

$$D = \left[6\left(Q_i + Q_o\right)/\left(\pi f\right)\right]^{1/3},$$
$$D_i = \left[6Q_i/\left(\pi f\right)\right]^{1/3}.$$

From the above formulas, it can be found that the generated double emulsion size is determined only by the two fluids flow rates and vibration frequency, but not to the physicochemical parameters of the fluids and the experimental setup. Similarly, the size of the inner core of the double emulsions is only related to the inner flow rate and vibration frequency, but not to other parameters. The sizes and shapes of the double emulsions can be precisely adjusted in a broad range of experimental parameters, as shown in **Figures 3A,B**. The black and red dots indicate the experimental results of the double emulsion shell and core diameters, respectively. The black and red solid lines refer to the theoretical curves of the double emulsion shell and core diameters, respectively. When the vibration frequency and the ratio of inner and outer flow rates ($\varphi = Q_i{:}Q_o$) remain constant, the sizes of the double emulsion shell and core increase with the increase of the total flow rate of the two fluids (**Figure 3A**). When the total flow rate and the ratio of inner and outer flow rates remain constant, the sizes of the double emulsion shell and core decrease with the increase of the vibration frequency (**Figure 3B**). In the experiment, the amplitude of the exciter is kept the same at different vibration frequencies by adjusting the excitation voltage. The relationship between the frequency and the voltage is obtained by a laser distance sensor when the vibration amplitude keeps at a constant. The data indicate that the experimental and theoretical values are in good agreement. Here, the maximum frequency of droplet generation can be up to around 40 Hz. However, with the further increase of vibration frequency, the droplet will fall from the coaxial needle before the fracture of liquid bridge, resulting in the failure of the CIS process [48, 49]. The maximum vibration frequency can be increased to a certain extent by reducing the geometric parameters of the coaxial needle.

Magnetic Guided Movement and Ultra Sound Activation of Perfluorocarbon-Loaded Magnetic Hydrogel Microcapsules

Iron oxide MNPs are dispersed in the shell of PMHMs which makes the hydrogel microcapsules can be attracted by the external magnetic field. **Figure 4A** illustrates the movement

process of the PMHMs in mineral oil under magnetic field. **Figure 4B** shows the change of PMHMs position with time under magnetic field (0.4 T) in a rectangular glass slot. The movement speed of the PMHMs gradually increases with time, mainly due to the gradual increase of magnetic attraction. In the first 10 s, the droplet only moves about half of the distance, but the second half only takes 2 s. The content of the MNPs in the shell, the intensity of the magnetic field and the distance between the magnet and the PMHMs all affect the movement of the PMHMs. For the movement of PMHMs, a video clip is available as Supplementary data (Supplementary Video 2). Because the PNIPAM shell has excellent flexibility characteristics, a certain deformation will occur when the PMHMs hit the wall surface, and the PMHMs' morphology will return to the original state after the magnetic field is canceled. These experimental results show that the prepared PMHMs have excellent magnetic response characteristics, and are expected to be used in magnetic controlled drug delivery.

US activation PFC droplet mainly relies on negative pressure to make droplets vaporize rapidly, and the time dimension is usually millisecond [6, 49]. Because the ultrasonic probe is relatively large, multiple PMHMs will be activated simultaneously during the US activation process, as illustrated in **Figure 5A**. **Figures 5B,C** show the changes of PMHMs before

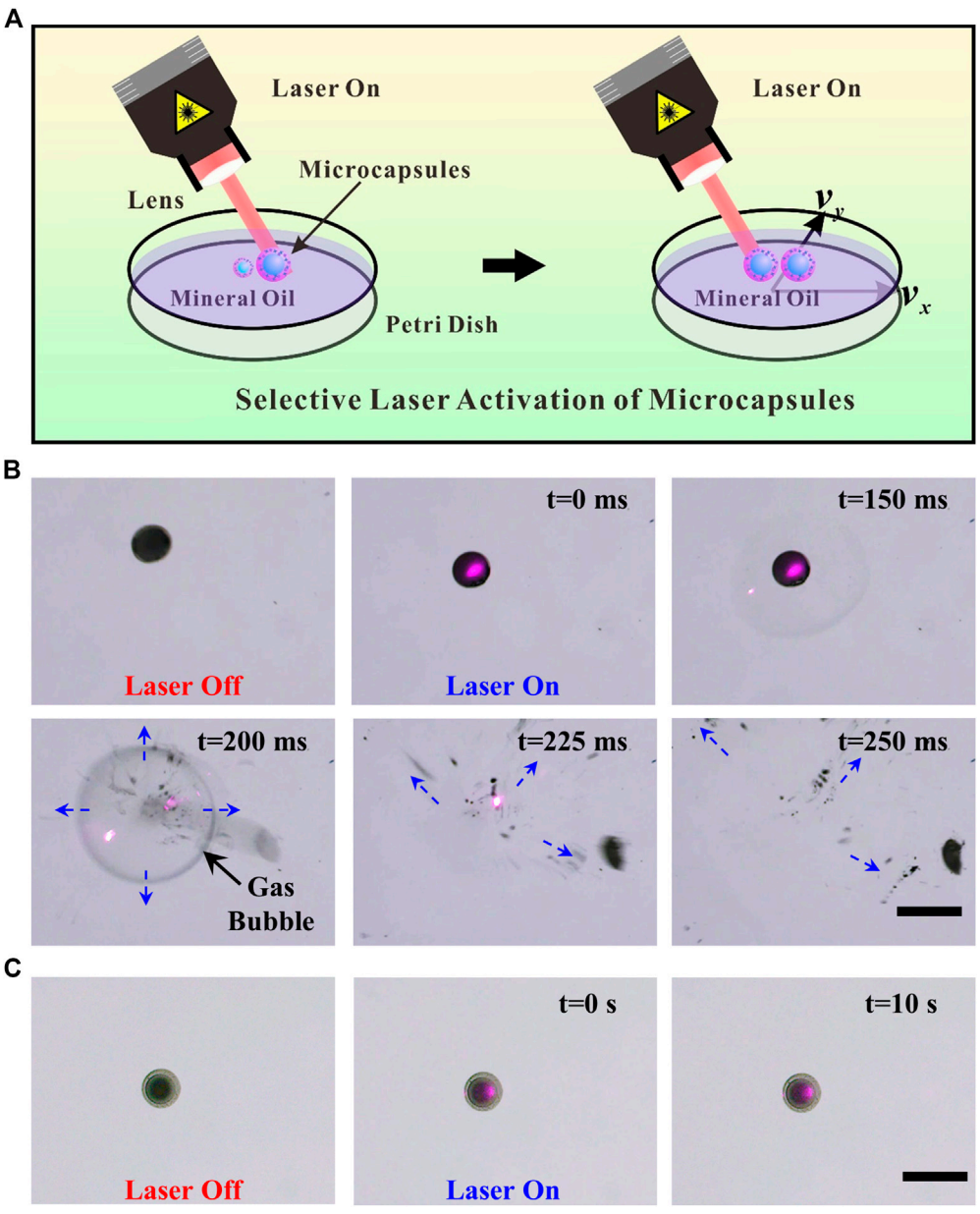

FIGURE 6 | (A) Schematic illustration of the laser activation of PMHMs. **(B)** Microscopic image of a single PMHM under NIR laser irradiation at different times. **(C)** Microscopic image of the produced PFC-loaded PNIPAM microcapsules without MNPs in the shell under NIR laser irradiation at different times. Scale bar: 500 μm.

and after US activation. Under the action of ultrasound (1 MHz, 45 s, 1.5 W/cm^2, duty cycle of 50%), the PNIPAM hydrogel shell breaks into debris as shown in **Figure 5C**. The experiment preliminarily verifies the feasibility of US activation of PMHMs, which lays a certain foundation for the application of the magnetic-controlled US responsive hydrogel microcapsules.

Laser Activation of Perfluorocarbon-Loaded Magnetic Hydrogel Microcapsules

Because iron oxide MNP is a kind of light-absorbing medium, a NIR laser with a wavelength of 808 nm is chosen to activate PMHMs. Under the focusing effect of the lens, the laser spot becomes smaller than the droplet diameter, so the laser has a better activation resolution, as illustrated in **Figure 6A**. The diameter of the focused laser spot is about 8 μm and the laser intensity is calculated to be 7.8×10^3 W/mm^2. The temperature of the focusing part on the microcapsule would exceed the vaporization temperature of PFC (55°C). **Figure 6B** shows the time sequence of a single PMHM under laser irradiation. Under the laser irradiation, PFC droplets vaporize rapidly and explode, which break the PNIPAM shell. The laser activation process is recorded as Supplementary data (Supplementary Video 3). At 200 ms, the PFC bubble explodes to generate a violent shock wave, which causes the fluid around the microcapsule to flow outward. After the explosion, the surrounding fluids will return to fill the vacant position. The blue arrows indicate the direction of fluid movement. As a contrast, the PFC-loaded hydrogel microcapsules without iron oxide MNPs are prepared to observe the changes of the microcapsules under laser irradiation. No changes have occurred after 10 s of laser irradiation (**Figure 6C**), further

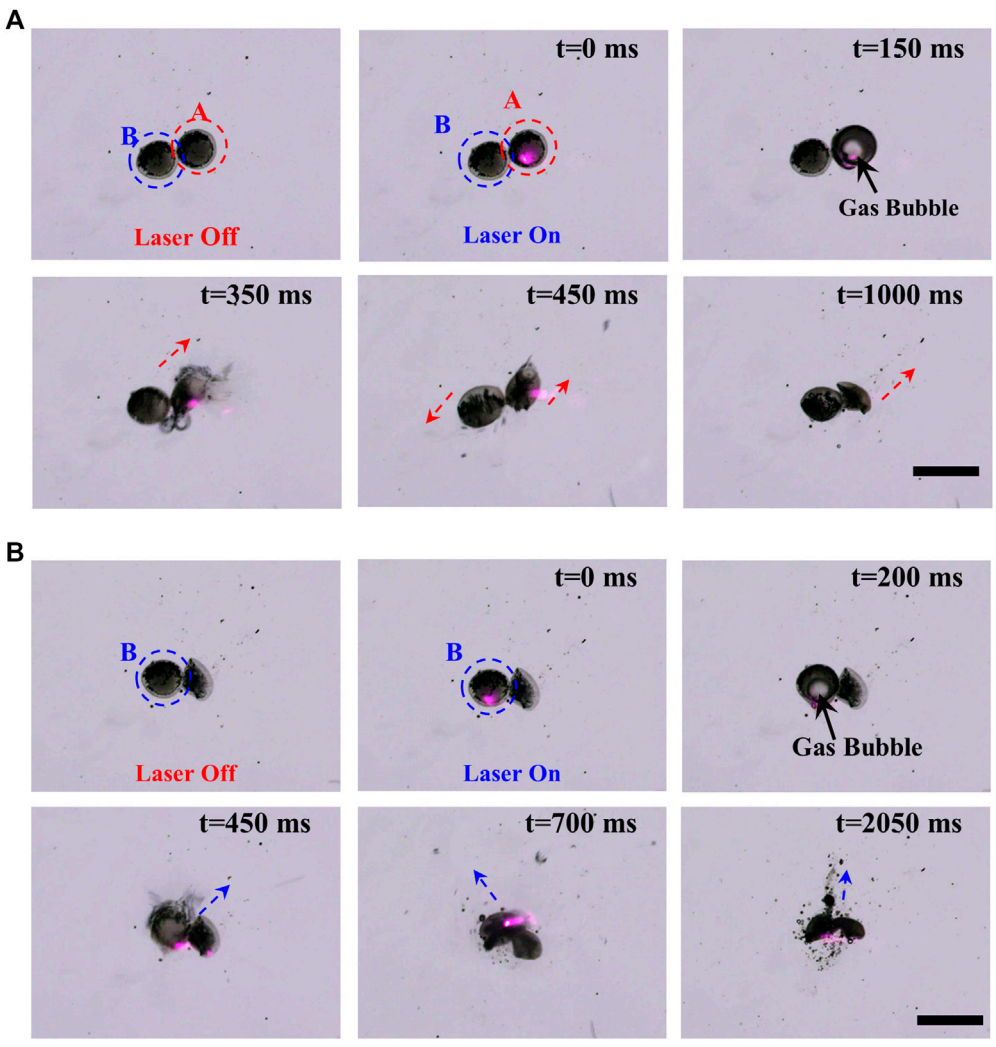

FIGURE 7 | Sequential laser activation of PMHMs. **(A)** NIR laser activation process of the first PMHM at different times. **(B)** NIR laser activation process of the second PMHM at different times. Scale bar: 500 μm.

confirming that the MNPs absorbing light energy and generating heat is the main reason for the vaporization of PFC core.

In the process of double emulsions crosslinking, if two droplets are very close together, they will adhere to each other after crosslinking. **Figures 7A,B** show the sequential laser activation process of two PMHMs attached to each other. The red and blue circles show the first and the second activated PMHMs. Because of the small laser spot, it is easy to realize the site-specific activation of the different PMHMs. The sequential laser activation process is recorded as Supplementary data (Supplementary Video 4). During the laser excitation process, the gas core is first generated in the PFC core and gradually increases and eventually ruptures [6], as indicated by the black arrows. The red and blue arrows indicate the different directions of debris movement. The experimental results show that the laser has the potential to achieve accurate drug delivery and release.

CONCLUSION

In summary, a simple, facile, and low-cost CIS technique was proposed to prepare uniform PMHMs for magnetic guided US and laser activation. Herein, the outer shell of PMHMs is PNIPAM combined with MNPs and the inner core is US-responsive PFC liquid which makes the PMHMs have magnetic-, US-, and photothermal-responsive characteristics. Moreover, the PMHMs have the potential to synergistic delivery of multiple distinct drugs. Additionally, the size, structure of the PMHM can be precisely adjusted in a wide range by controlling the experimental parameters. US and laser activation of PMHMs have been verified by a series of experiments, US has the potential to quickly release multiple PMHMs, while laser has the ability to activate PMHMs more accurately. The PMHMs have excellent magnetic-response characteristics which can further improve the controllability of drug release. It can be concluded that the produced uniform PMHMs may have great application potential in biomedicine, engineering, chemistry, material science, and other fields.

DATA AVAILABILITY STATEMENT

The original contributions presented in the study are included in the article/**Supplementary Material**, further inquiries can be directed to the corresponding author/s.

AUTHOR CONTRIBUTIONS

ZZ designed and carried out the experiment, collected and analyzed the data and wrote the manuscript. MZ, YZ, and FH assisted the experiment. TS and RX guided the research and revised the manuscript. All authors contributed to manuscript revision, read, and approved the submitted version.

FUNDING

This work was supported by the National Natural Science Foundation of China (Nos. 11722222, 11621202), the Strategic Priority Research Program of the Chinese Academy of Sciences (No. XDB22040403), the Anhui Provincial Natural Science Foundation (1908085QE200), the Youth Innovation Promotion Association CAS (No. 2018491), and the Fundamental Research Funds for the Central Universities.

SUPPLEMENTARY MATERIAL

The Supplementary Material for this article can be found online at: https://www.frontiersin.org/articles/10.3389/fphy.2020.581519/full#supplementary-material

Supplementary Video 1: CIS double emulsions preparation process (MP4).

Supplementary Video 2: Magnetic controlled movement of PMHMs (MP4).

Supplementary Video 3: Laser activation of a single PMHM (MP4).

Supplementary Video 4: Sequential laser activation process of two PMHMs (MP4).

REFERENCES

1. Zhao CX. Multiphase flow microfluidics for the production of single or multiple emulsions for drug delivery. *Adv Drug Deliv Rev* (2013) **65**(11–12):1420–46. doi:10.1016/j.addr.2013.05.009
2. He F, Zhang M-J, Wang W, Cai Q-W, Su Y-Y, Liu Z, et al. Designable polymeric microparticles from droplet microfluidics for controlled drug release. *Adv Mater Technol* (2019) **4**(6):1800687. doi:10.1002/admt.201800687
3. Lengyel M, Kallai-Szabo N, Antal V, Laki AJ, Antal I. Microparticles, microspheres, and microcapsules for advanced drug delivery. *Sci Pharm* (2019) **87**(3):20. doi:10.3390/scipharm87030020
4. Zhang Y, Yu J, Bomba HN, Zhu Y, Gu Z. Mechanical force-triggered drug delivery. *Chem Rev* (2016) **116**(19):12536–63. doi:10.1021/acs.chemrev.6b00369
5. Zhang A, Jung K, Li A, Liu J, Boyer C. Recent advances in stimuli-responsive polymer systems for remotely controlled drug release. *Prog Polym Sci* (2019) **99**: 101164. doi:10.1016/j.progpolymsci.2019.101164
6. Zhu Z, Wu Q, Li G, Han S, Si T, Xu RX. Microfluidic fabrication of stimuli-responsive microdroplets for acoustic and optical droplet vaporization. *J Mater Chem B* (2016) **4**(15):2723–30. doi:10.1039/c5tb02402a
7. Si T, Li G, Wu Q, Zhu Z, Luo X, Xu RX. Optical droplet vaporization of nanoparticle-loaded stimuli-responsive microbubbles. *Appl Phys Lett* (2016) **108**(11):111109. doi:10.1063/1.4944539
8. Duarte ARC, Ünal B, Mano JF, Reis RL, Jensen KF. Microfluidic production of perfluorocarbon-alginate core-shell microparticles for ultrasound therapeutic applications. *Langmuir* (2014) **30**(41):12391–9. doi:10.1021/la502822v
9. Soto F, Martin A, Ibsen S, Vaidyanathan M, Garcia-Gradilla V, Levin Y, et al. Acoustic microcannons: toward advanced microballistics. *ACS Nano* (2016) **10**(1):1522–8. doi:10.1021/acsnano.5b07080
10. Dwivedi P, Kiran S, Han S, Dwivedi M, Khatik R, Fan R, et al. Magnetic targeting and ultrasound activation of liposome-microbubble conjugate for enhanced delivery of anti-cancer therapies. *ACS Appl Mater Interfaces* (2020) **12**:23737–23751. doi:10.1021/acsami.0c05308

11. Sun Y, Wang Y, Niu C, Strohm EM, Zheng Y, Ran H, et al. Laser-activatible PLGA microparticles for image-guided cancer therapy in vivo. *Adv Funct Mater* (2014) **24**(48):7674–80. doi:10.1002/adfm.201402631
12. Wilson K, Homan K, Emelianov S. Biomedical photoacoustics beyond thermal expansion using triggered nanodroplet vaporization for contrast-enhanced imaging. *Nat Commun* (2012) **3**:618. doi:10.1038/ncomms1627
13. Gao D, Xu M, Cao Z, Gao J, Chen Y, Li Y, et al. Ultrasound-Triggered phase-transition cationic nanodroplets for enhanced gene delivery. *ACS Appl Mater Interfaces* (2015) **7**(24):13524–37. doi:10.1021/acsami.5b02832
14. Lee TY, Choi TM, Shim TS, Frijns RAM, Kim S-H. Microfluidic production of multiple emulsions and functional microcapsules. *Lab Chip* (2016) **16**(18):3415–40. doi:10.1039/c6lc00809g
15. Shang L, Cheng Y, Zhao Y. Emerging droplet microfluidics. *Chem Rev* (2017) **117**(12):7964–8040. doi:10.1021/acs.chemrev.6b00848
16. Wang J, Eijkel JCT, Jin M, Xie S, Yuan D, Zhou G, et al. Microfluidic fabrication of responsive hierarchical microscale particles from macroscale materials and nanoscale particles. *Sensor Actuator B Chem* (2017) **247**:78–91. doi:10.1016/j.snb.2017.02.056
17. Li W, Zhang L, Ge X, Xu B, Zhang W, Qu L, et al. Microfluidic fabrication of microparticles for biomedical applications. *Chem Soc Rev* (2018) **47**(15):5646–83. doi:10.1039/c7cs00263g
18. Zhao Q, Cui H, Wang Y, Du X. Microfluidic platforms toward rational material fabrication for biomedical applications. *Small* (2019) **16**(9):e1903798. doi:10.1002/smll.201903798
19. Utada AS, Lorenceau E, Link D, Kalpan PD, Stone HA, Weitz DA. Monodisperse double emulsions generated from a microcapillary device. *Science* (2005) **308**(5721):537–41. doi:10.1126/science.1109164
20. Bell RV, Parkins CC, Young RA, Preuss CM, Stevens MM, Bon SAF. Assembly of emulsion droplets into fibers by microfluidic wet spinning. *J Mater Chem* (2016) **4**(3):813–8. doi:10.1039/c5ta08917d
21. Chaurasia AS, Sajjadi S. Flexible asymmetric encapsulation for dehydration-responsive hybrid microfibers. *Small* (2016) **12**(30):4146–55. doi:10.1002/smll.201600465
22. Chen A, Ge X-h, Chen J, Zhang L, Xu J-H. Multi-functional micromotor: microfluidic fabrication and water treatment application. *Lab Chip* (2017) **17**(24):4220–4. doi:10.1039/c7lc00950j
23. Shang L, Wang Y, Yu Y, Wang J, Zhao Z, Xu H, et al.. Bio-inspired stimuli-responsive graphene oxide fibers from microfluidics. *J Mater Chem* (2017) **5**(29):15026–30. doi:10.1039/c7ta02924a
24. Meng Z-J, Zhang J, Deng X, Liu J, Yu Z, Abell C. Bioinspired hydrogel microfibres colour-encoded with colloidal crystals. *Mater Horiz* (2019) **6**:1938–43. doi:10.1039/C9MH00528E
25. Anna SL, Bontoux N, Stone HA. Formation of dispersions using "flow focusing" in microchannels. *Appl Phys Lett* **82**(3):364–6. doi:10.1063/1.1537519
26. Chan HF, Zhang Y, Leong KW. Efficient one-step production of microencapsulated hepatocyte spheroids with enhanced functions. *Small* (2016) **12**(20):2720–30. doi:10.1002/smll.201502932
27. Li D, Li X, Chen C, Zheng Z, Chang H. Monodisperse water-in-oil-in-water emulsions generation for synthesising alginate hydrogel microspheres *via* locally hydrophobic modification to PMMA microchannels. *Sensor Actuator B Chem* (2018) **255**:1048–56. doi:10.1016/j.snb.2017.08.152
28. Zhang L, Chen K, Zhang H, Pang B, Choi C-H, Mao AS, et al. Microfluidic templated multicompartment microgels for 3D encapsulation and pairing of single cells. *Small* (2018) **14**(9):1702955. doi:10.1002/smll.201702955
29. Guerzoni LPB, Rose JC, Gehlen DB, Jans A, Haraszti T, Wessling M, et al. Cell encapsulation in soft, anisometric poly(ethylene) glycol microgels using a novel radical-free microfluidic system. *Small* (2019) **15**(20):e1900692. doi:10.1002/smll.201900692
30. Samandari M, Alipanah F, Javanmard SH, Sanati-Nezhad A. One-step wettability patterning of PDMS microchannels for generation of monodisperse alginate microbeads by in situ external gelation in double emulsion microdroplets. *Sens Actuators B Chem* (2019) **291**:418–25. doi:10.1016/j.snb.2019.04.100
31. Zhu Z, Si T, Xu RX. Microencapsulation of indocyanine green for potential applications in image-guided drug delivery. *Lab Chip* (2015) **15**(3):646–9. doi:10.1039/c4lc01032a
32. Si T, Yin C, Gao P, Ding H, Li GB, He XM, et al. Steady cone-jet mode in compound-fluidic electro-flow focusing for fabricating multicompartment microcapsules. *Appl Phys Lett* (2016) **108**(2):021601. doi:10.1063/1.4939632
33. Wu Q, Yang C, Liu G, Xu W, Zhu Z, Si T, et al. Multiplex coaxial flow focusing for producing multicompartment Janus microcapsules with tunable material compositions and structural characteristics. *Lab Chip* (2017) **17**(18):3168–75. doi:10.1039/c7lc00769h
34. Wu Q, Yang C, Yang J, Huang F, Liu G, Zhu Z, et al. Photopolymerization of complex emulsions with irregular shapes fabricated by multiplex coaxial flow focusing. *Appl Phys Lett* (2018) **112**(7):071601. doi:10.1063/1.5018207
35. Zhu Z, Wu Q, Han S, Xu W, Zhong F, Yuan S, et al. Rapid production of single- and multi-compartment polymeric microcapsules in a facile 3D microfluidic process for magnetic separation and synergistic delivery. *Sensor Actuator B Chem* (2018) **275**:190–8. doi:10.1016/j.snb.2018.08.044
36. Zhong F, Yang C, Wu Q, Wang S, Cheng L, Dwivedi P, et al. Preparation of pesticide-loaded microcapsules by liquid-driven coaxial flow focusing for controlled release. *Int J Polym Mater* (2019) **69**:840–7. doi:10.1080/00914037.2019.1617710
37. Yang C, Qiao R, Mu K, Zhu Z, Xu R, Si T, et al. Manipulation of jet breakup length and droplet size in axisymmetric flow focusing upon actuation. *Phys Fluids* (2019) **31**(9):091702. doi:10.1063/1.5122761
38. Liu G, Wu Q, Dwivedi P, Hu C, Zhu Z, Shen S, et al. Hemoglobin-laden microcapsules for simulating oxygen dynamics of biological tissue. *ACS Biomater Sci Eng* (2018) **4**(9):3177–84. doi:10.1021/acsbiomaterials.8b00830
39. Dwivedi P, Yuan S, Han S, Mangrio FA, Zhu Z, Lei F, et al. Core–shell microencapsulation of curcumin in PLGA microparticles: programmed for application in ovarian cancer therapy. *Artif Cells Nanomed Biotechnol* (2018) S481–91. doi:10.1080/21691401.2018.1499664
40. Martino C, Berger S, Wootton RCR, deMello AJ. A 3D-printed microcapillary assembly for facile double emulsion generation. *Lab Chip* (2014) **14**(21):4178–82. doi:10.1039/c4lc00992d
41. Waheed S, Cabot JM, Macdonald NP, Lewis T, Guijt RM, Paull B, et al. 3D printed microfluidic devices: enablers and barriers. *Lab Chip* (2016) **16**(11):1993–2013. doi:10.1039/c6lc00284f
42. Weisgrab G, Ovsianikov A, Costa PF. Functional 3D printing for microfluidic chips. *Adv Mater Technol* (2019) **4**(10):1900275. doi:10.1002/admt.201900275
43. Nielsen AV, Beauchamp MJ, Nordin GP, Woolley AT. 3D printed microfluidics. *Annu Rev Anal Chem* (2020) **13**(1):45–65. doi:10.1146/annurev-anchem-091619-102649
44. Gu H, Duits MHG, Mugele F. Droplets formation and merging in two-phase flow microfluidics. *Int J Mol Sci* (2011) **12**(4):2572–97. doi:10.3390/ijms12042572
45. Si T, Li F, Yin X-Y, Yin X-Z. Modes in flow focusing and instability of coaxial liquid-gas jets. *J Fluid Mech* (2009) **629**:1–23. doi:10.1017/s0022112009006211
46. Ganan-Calvo AM, Montanero JM, Martin-Banderas L, Flores-Mosquera M. Building functional materials for health care and pharmacy from microfluidic principles and flow focusing. *Adv Drug Deliv Rev* (2013) **65**(11-12):1447–69. doi:10.1016/j.addr.2013.08.003
47. Zhu P, Wang L, Passive and active droplet generation with microfluidics: a review. *Lab Chip* (2017) **17**(1):34–75. doi:10.1039/c6lc01018k
48. Huang F, Zhu Z, Niu Y, Zhao Y, Si T, Xu RX. Coaxial oblique interface shearing: tunable generation and sorting of double emulsions for spatial gradient drug release. *Lab Chip* (2020) **20**(7):1249–1258. doi:10.1039/d0lc00111b.
49. Zhu Z, Huang F, Yang C, Si T, Xu RX. On-demand generation of double emulsions based on interface shearing for controlled ultrasound activation. *ACS Appl Mater Interfaces* (2019) **11**(43):40932–43. doi:10.1021/acsami.9b15182

Conflict of Interest: The authors declare that the research was conducted in the absence of any commercial or financial relationships that could be construed as a potential conflict of interest.